Laser Physics, Vol. 15, No. 1, 2005, pp. 195–204.

Attosecond Metrology with Controlled Light Waveforms

M. Uiberacker[1, *], E. Goulielmakis[1], R. Kienberger[1], A. Baltuska[1], T. Westerwalbesloh[2], U. Keineberg[2], U. Heinzmann[2], M. Drescher[2], and F. Krausz[1, 3]

[1] *Institut für Photonik, Technische Universität Wien, Gusshausstr. 27, A-1040 Wien, Austria*
[2] *Fakultät für Physik, Universitat Bielefeld, D-33615 Bielefeld, Germany*
[3] *Max-Planck-Institut für Quantenoptik, Hans-Kopfermann-Strasse 1, D-85748 Garching, Germany*
*e-mail: uiberacker@mpq.mpg.de
Received September 2, 2004

Abstract—The electric field oscillations of visible light change their sign about 10^{15} times per second, and, therefore, the field strength changes from zero to maximum in less than a femtosecond (10^{-15} s). By precisely controlling these oscillations within a very short laser pulse, we were able to demonstrate an apparatus capable of measuring atomic processes with an accuracy of approximately 100 attoseconds (10^{-18} s). A controlled, intense 5-femtosecond laser pulse is used to create a 250-attosecond x-ray pulse that triggers the atomic process. The electric field oscillations of the same laser pulse are used to probe the time structure of the process. This measuring technique allows for the tracing of very fast processes in the electron shells of atoms for the first time.

Increasing the accuracy of measurements of time has always been a challenge to science and has made it possible to explore short-lived phenomena that hitherto could not be measured. Recently, femtosecond laser techniques have allowed for the tracing and control of molecular dynamics and the related motion of atoms on the length scale of internuclear separations without the need for resolving the particles' positions in space [1]. Here, we demonstrate the possibility of exploring the microcosm even further, to the interior of atoms and thus to electronic processes on an attosecond timescale.

As direct measurements of the time evolution of ultrafast processes are not feasible, one has to sample the evolution point by point with reproducible conditions (pump/probe technique). This implies the reproducible generation of a trigger (pump pulse) for the process under investigation, as well as an event for probing the state of the process (probe pulse), where the duration of the trigger and probe and the accuracy of the timing between the pump and probe event determine the time resolution of the measurement. Traditionally, the fastest measurement techniques have used the envelope of laser pulses of visible light, with durations of around 5 femtoseconds (1 fs = 10^{-15} s) for sampling [3, 4, 5]. Recently, sub-femtosecond bunching of femtosecond (>10 fs) extreme-ultraviolet light (XUV) was observed in two-color [6, 7] and two-photon [8] ionization experiments, and evidence of sub-femtosecond confinement of XUV emission from few-cycle-driven (ionizing) atoms was obtained [9]. However, time-domain measurements have not been capable of resolving the time structures of sub-femtosecond transients.

The apparatus explained here extends these capabilities to a resolution within the Bohr orbit time, which is about 150 as. The technique draws on the basic operation principle of a streak camera [10–14] (Fig. 1), where a light pulse generates an electron bunch with an identical temporal structure. The electrons are transversally deflected by an electric field as they travel to the detector screen. From the streaked image of the photoelectron bunch, it is possible to infer, with sub-picosecond resolution, the temporal structure of the light pulse that triggered the photoemission. The time resolution of these devices is ultimately limited by the spread of the electron transit time due to a spread in their initial momenta.

In this work, we report the temporal characterization of sub-femtosecond electron emission from atoms by drawing on the same basic concept. We use an accurately controlled few-cycle wave of visible light to take "streaked images" of the time–momentum distribution of electrons ejected from atoms due to sudden excitation (e.g., by an isolated attosecond electron or photon burst synchronized to the light wave). From these images, this technique—the atomic transient recorder (ATR) [15]—can measure the temporal evolution of the spectrally resolved intensity of emitted (primary and secondary) electrons and, therefore, provides direct temporal insight into the rearrangement of the electronic shells of excited atoms on a sub-femtosecond timescale.

ATTOSECOND SOFT-X-RAY PULSES

If the electric field of linearly-polarized femtosecond laser pulses is sufficiently strong, it induces—in a highly nonlinear interaction—gigantic dipole oscillations in atoms by pulling an electron away from the core and smashing it back half a cycle later. These oscillations are not sinusoidal; they contain very-high-frequency components extending into the extreme-

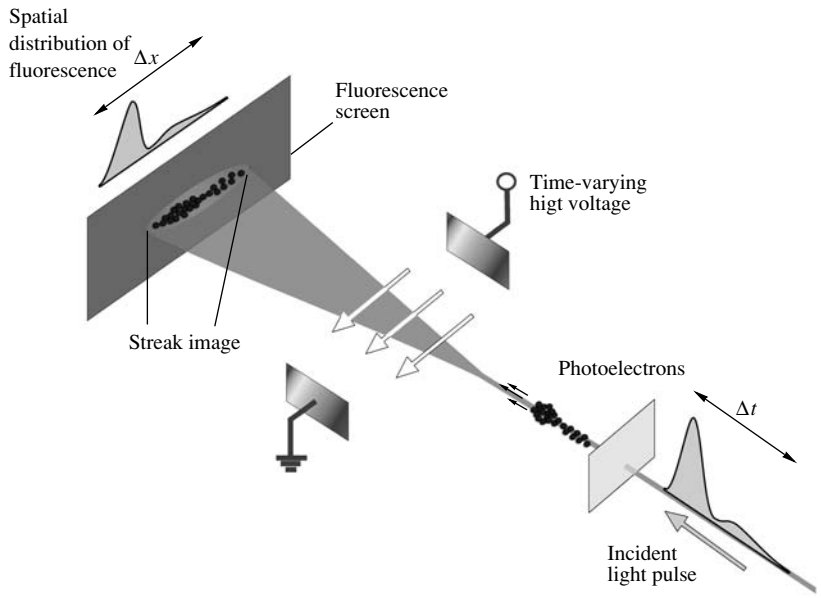

Fig. 1. Principle of conventional streak camera. A light flash hits a photocathode and induces electron emission. The electrons travel towards the phosphorous screen, while a rapidly increasing high voltage tranversally deflects them. The time duration (Δt) of the incident light flash can be unambiguously inferred from the width of the streaked image on the screen (Δx). The faster the deflecting field varies, the shorter the pulses that can be recorded. The best resolution is about 100 femtoseconds.

ultraviolet and soft-X-ray regimes [3]. In a laser field containing many oscillation cycles, the oscillations are repeated quasi-periodically, resulting in the emission of a series of high-energy bursts of sub-femtosecond duration and high-order harmonics of the laser radiation in the spectral domain. For a few-cycle laser driver, only a few dipole oscillations with different amplitudes occur. Only the oscillation with the highest amplitude has been predicted to emit the highest photon energies, and, therefore, the highest spectral components are confined to a single burst in the time domain [2].

The first evidence of emission of an isolated sub-femtosecond pulse from this interaction was reported in 2001 [9], but reproducible generation of single sub-femtosecond pulses did not become possible till 2003, when the waveform of intense few-cycle laser pulses could be precisely controlled [2]. Since then, the giant atomic-dipole oscillations can be controlled and reproduced in every laser shot. With the parameters set correctly, this leads to the generation of a single X-ray burst with parameters of duration, energy, and timing with respect to the laser field that are well reproduced from one shot to the next. Synchronism of the X-ray burst to the field oscillations of the generating laser pulse affords the potential for using the X-ray burst for attosecond spectroscopy by utilizing the oscillating laser field as a probe. This is essential because—due to the unfavorable scaling of two-photon transition cross sections with the photon energy—these laser-produced X-ray bursts are too weak to be used for *both* triggering *and* probing electronic dynamics (X-ray-pump/X-ray-probe spectroscopy). Instead, the oscillating laser field, which changes its strength from zero to a maximum within some 600 attoseconds in a 750-nm laser wave, can take over the role of the probing X-ray pulse.

RESOLVING ATOMIC TRANSIENTS

Today's image-tube streak cameras allow for electron-optical chronoscopy with sub-picosecond resolution [11, 12]. The ATR provides a three-orders-of-magnitude improvement in time resolution that results from several essential modifications of image-tube streak cameras: (i) the electric field of light is used to affect the motion of the electrons; the field is (ii) virtually jitter-free, (iii) acting along the direction of electron motion (implying their acceleration or deceleration instead of their deflection), and (iv) applied directly at the location and instant of emission. Whereas (i) implies "only" a dramatically enhanced streaking speed, the consequences of (ii)–(iv) are much more profound: (ii) allows for the timing of the probing field to be systematically varied with an accuracy within the electron bunch length, and thanks to (iii) this capability results in a "projecting" of the initial time–momentum distribution of the electron emission into a series of different final (measurable) momentum distributions, while (iv) prevents the initial momentum spread from introducing any measurement error.

Inspired by the physics of the first sub-femtosecond experiment [9], Corkum and coworkers [13] put forward the basic concept for ATR metrology, and it was analyzed with a comprehensive quantum theory by Brabec and coworkers [14]. Let us consider electron

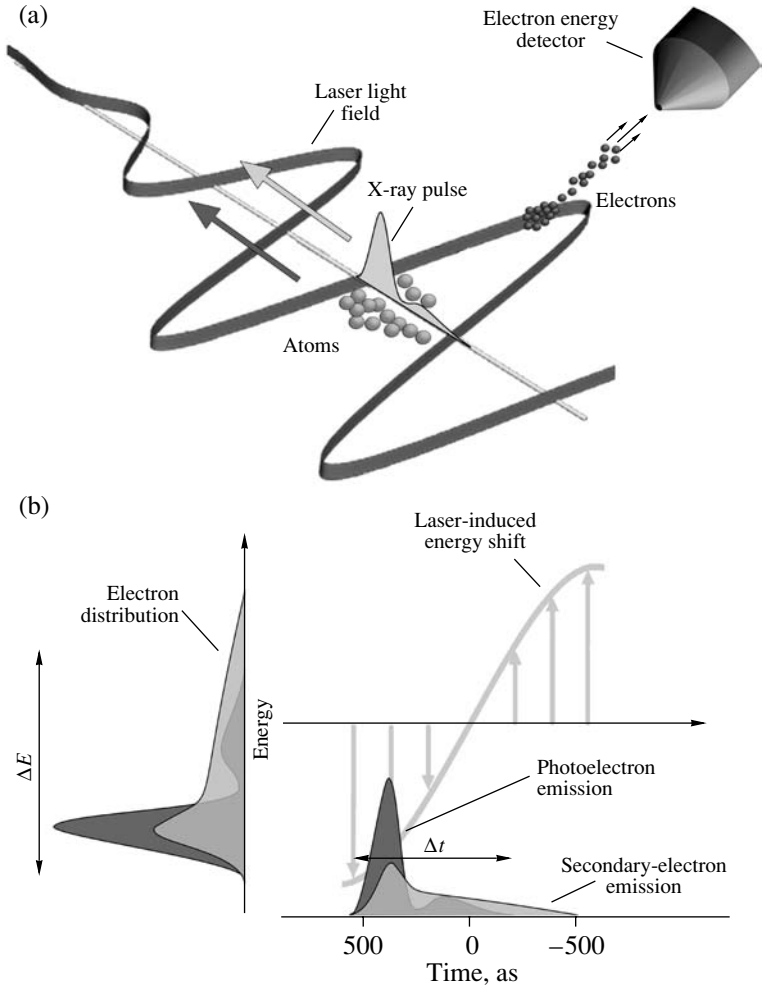

Fig. 2. Principle of light-field-controlled streak camera. (a) A bunch of atoms are exposed simultaneously to a sub-femtosecond X-ray flash and a laser pulse consisting of a few well-controlled field oscillations. The kinetic energy of electrons emitted by the X-ray flash in the direction of laser polarization is detected with a time-of-flight electron detector. Depending on their time of birth within the half period of the light-field oscillations, the kinetic energy of the electrons is increased or decreased by interaction with the laser field. (b) Projection of the hypothetical temporal emission profile of photo and Auger electrons to final energy distributions. The width (ΔE) and shape of the electron energy distributions mirror the duration (Δt) and evolution of the emission within half a cycle.

emission from atoms exposed to a sub-fs X-ray burst in the presence of an intense, linearly-polarized, few-cycle laser field $E_L(t) = E_0(t)\cos(\omega_L t + \varphi)$. The momentum of the freed electrons is changed by $\Delta p = eA_L(t)$ along the laser field vector (Fig. 2). Here, $A_L(t_r) = \int_{t_r}^{\infty} E_L(t)dt$ is the vector potential of the laser field, e and m stand for the charge and rest mass of the electron, respectively, and t_r is the release time of the electron. This momentum transfer (gray arrows in Fig. 3) maps the temporal emission profile onto a similar distribution of final momenta $p_f = p_i + \Delta p$ within a time window of $T_0/2 = \pi/\omega_L$ if the electrons initial momentum p_i is constant in time and their emission terminates within $T_0/2$. Under these conditions, the temporal evolution of the electron emission can be unambiguously retrieved from a single "streaked" momentum distribution. However, any sweep of the electron's initial momentum revokes the unique correspondence between the electron's final momentum and the release time, preventing any retrieval of accurate temporal information from single-streak records (violet and orange profiles in Fig. 3).

In general, the initial momentum spectrum of electrons detached from atoms by impulsive excitation varies in time during emission. A representative time–momentum distribution $n_e(p, t)$ of the electron emission rate is depicted in Fig. 4. The final electron momentum spectrum (observed after the laser pulse has left the interaction region), $\sigma(p) = \int_{-\infty}^{\infty} n_e(p, t)dt$, can be viewed as the projection of the time-dependent momentum distribution on momentum space along lines of constant p. In the classical description of the motion of the freed

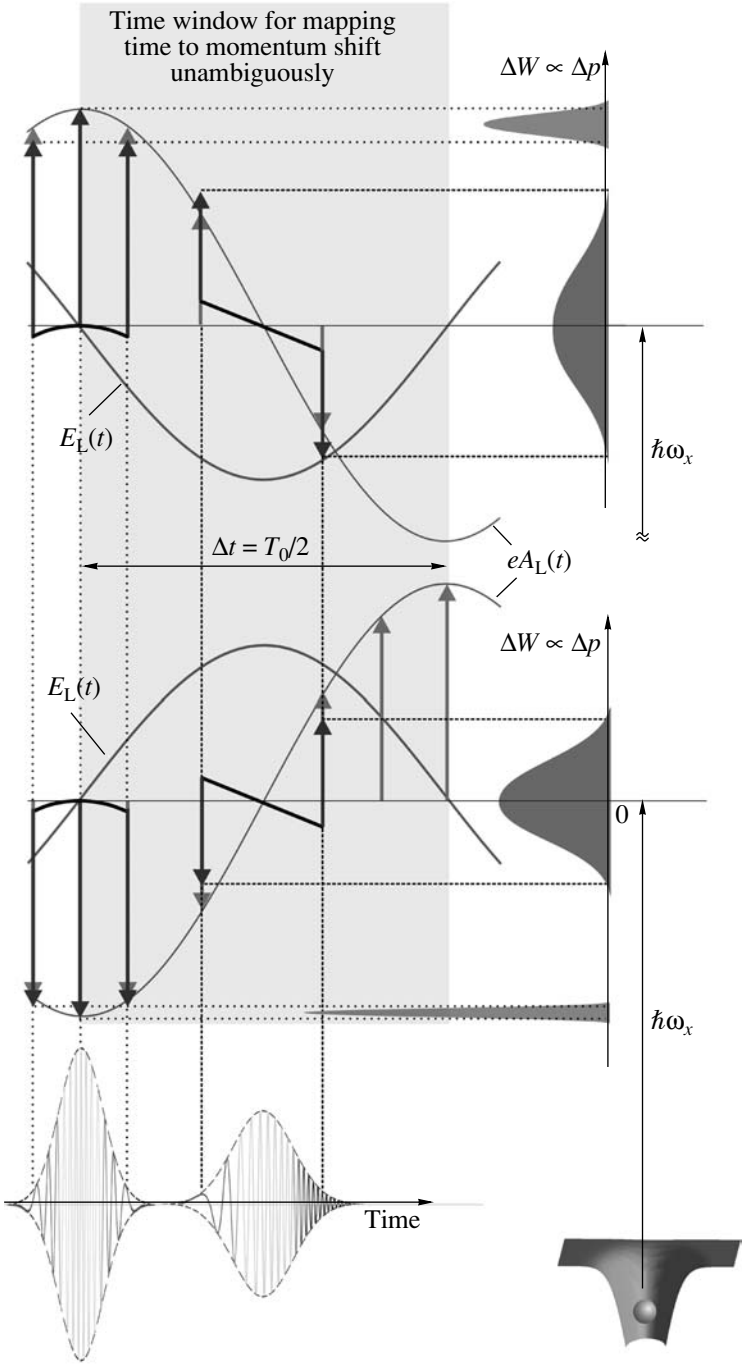

Fig. 3. Influence of a possible momentum sweep on measured spectra for two particular delays between electron emission and light oscillations. In the absence of a sweep, electrons emitted within the marked time window feel an additional momentum $\Delta p = eA_L(t)$ (gray oscillation and gray arrows). Their time distribution is mapped to the energy scale with $eA_L(t)$ as a transfer function. If a linear momentum sweep is present, the transfer function is influenced (tilted black lines and violet arrows), which results in a difference in the mapped spectra measured at different delays (violet spectra), from which the sweep can be evaluated. Even higher order momentum sweeps can be retrieved (curved black lines and orange spectra) for a changed delay position around the zero crossing of $E(t)$.

electrons in the presence of a strong laser field, the final spectra obtained are generalized projections along the lines where $p_f = p_i + eA_L(t)$ is constant (see Fig. 4). By repeating the measurement at different delays of the laser field with respect to the excitation that triggers electron emission, we obtain a suitable set of streaked spectra:

$$\sigma_A(p) = \int_{-\infty}^{\infty} n_e(p - eA_L(t), t)dt, \qquad (1)$$

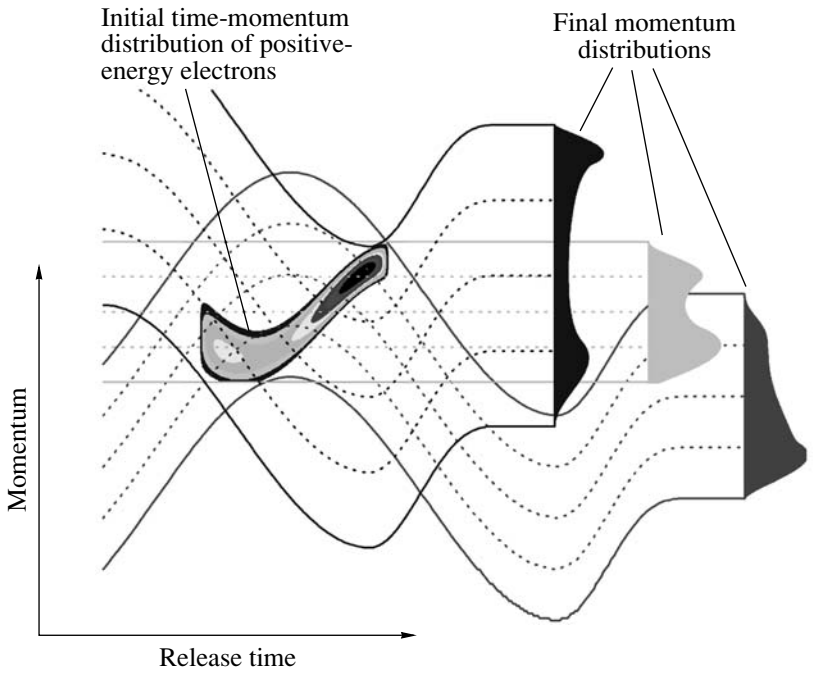

Fig. 4. Time-dependent momentum transfer to positive-energy electrons within the laser cycle. Electrons emitted from an excited atom along the electric field vector of a strong laser field with an initial momentum p_i suffer a momentum change that is proportional to the vector potential of the field $A_L(t)$ at the instant of release. For a certain time-momentum distribution, this will result in different "projection" spectra for different delays of the light oscillations. With a suitable set of spectra, the time-momentum distribution can be reconstructed.

from which the complete distribution $n_e(p, t)$ can be reconstructed. The method is closely related to frequency-resolved optical gating [15, 16] with the oscillating field as gate. In the simplest cases, such as in the absence of a nonlinear momentum sweep, the streak records obtained near the zero transitions of $A_L(t)$ with opposite slopes (violet profiles in Fig. 3) together with the field-free spectrum allow for the determination of all relevant characteristics: the temporal profile and the duration and momentum chirp of the emission. We note that a linear momentum sweep leads to differently broadened streaked spectra at these delays and that this difference makes the measurement highly sensitive to the momentum sweep, i.e., highly sensitive to deviations of the pulse duration from the Fourier limit.

The ATR's potential for determining a high-order chirp of the X-ray pulse as well is indicated by the different shapes of the momentum distributions (orange) in Fig. 3.

EXPERIMENTAL SETUP

We utilize the same experimental setup that was used to study photoelectrons [9] and that was recently employed for probing Auger electrons on a few-femtosecond time scale [17]. The essential innovation here is that waveform-controlled few-cycle light now provides a reproducible excitation burst for accurate triggering, as well as a reproducible streaking field for capturing sub-fs electron emission from atoms. The X-ray bursts for triggering are produced from Ne atoms ionized by intense, few-cycle waveform-controlled light pulses [2] in the process of high-order harmonic generation [18, 19]. The X-ray pulses copropagate with the laser pulses down the beam delivery tube (Fig. 5). After 150 cm, they hit a 200-nm-thick zirconium foil with an aperture of 2 mm mounted on a nitrocellulose membrane that is 5 μm thick. This virtually dispersionless filter produces an annular laser beam with the X-ray beam in the center. The energy in the laser beam is adjusted by a motorized iris and measured by a photodiode. The collinear X-ray and laser beams are focused into a second neon gas jet and delayed with respect to each other for the ATR measurements with a two-component Mo/Si broadband multilayer mirror (radius of curvature = −70 mm) placed 2 m downstream from the source. The reflectivity band of the multilayer extends from 85 to 100 eV with a peak reflectance of ~30% and a full width at half-maximum (FWHM) of ~9 eV. This mirror is mounted on a motorized stage so that it can be removed from the beam line. In this way, the harmonic beam can be detected by an X-ray CCD camera for optimizing the radial intensity profile of the X-ray beam. Further on, a 10000 lines/mm transmission grating can be inserted before the X-ray CCD camera to observe the spectrum of the harmonic radiation. Fine tuning of the cutoff of the X-rays can be carried out by fine tuning of the energy of the fundamental laser beam.

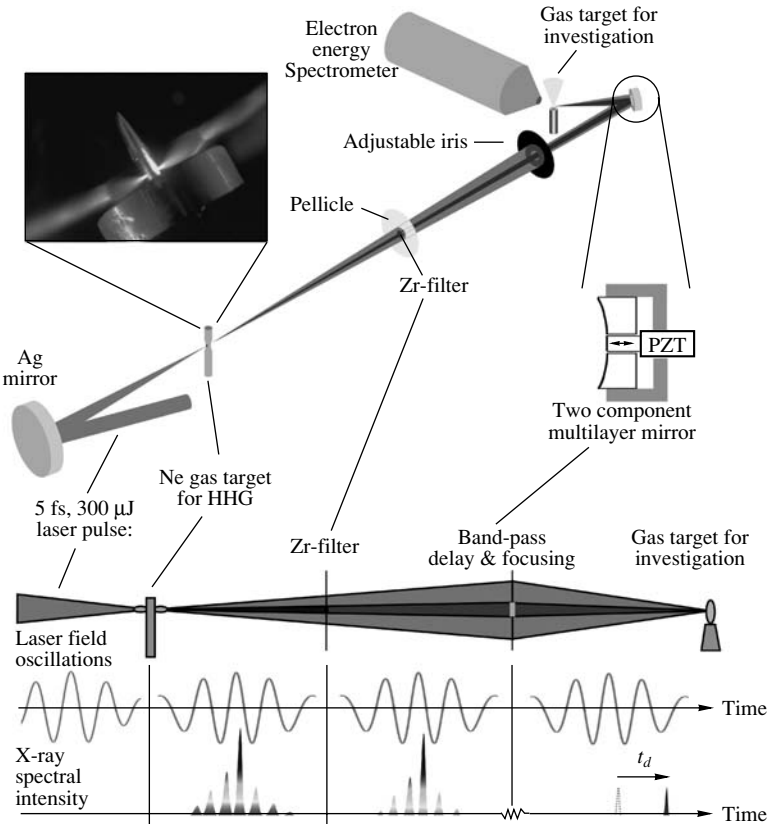

Fig. 5. Experimental setup of the evacuated beam line. The upper part depicts the schematic layout of the components and the lower part illustrates their function. The 5-fs visible laser pulses are focused into a Ne gas jet to create a few high-photon-energy (X-ray) bursts (the inset picture shows plasma clouds effusing from the interaction region). They are passed through a high-pass filter (Zr foil) to block laser light and the low-energy part of the bursts. Subsequently, the multilayer mirror unit selects only the highest energy spectral components of the X-ray radiation, which are confined to a single X-ray burst. The mirror unit can also be used to introduce a delay between the X-ray burst and laser pulse and focuses the two beams into the second gas target for implementing the light-field-controlled streak camera measurements.

Two types of experiments based on the ATR concept were implemented. First, the inner part of the Mo/Si mirror was used to focus both the X-ray and the laser beam to eliminate any external source of fluctuations in the timing between the excitation and probing pulses (Zr filter removed). In the second type of study, the X-ray beam was reflected by the inner part and the laser by the outer part of the mirror: the central piece sits on a piezo stage that is adjustable in the transverse and longitudinal directions. Thus, the two pulses can be overlapped spatially and temporally in the focal plane, exactly at the tip of a nozzle emitting the atoms to be studied. The time delay of the X-ray and the laser pulse can be varied with a piezo stage with nanometer precision.

Electrons ejected following the X-ray excitation are collected within a narrow cone (<4°) aligned parallel to the laser and X-ray polarization and analyzed with a time-of-flight spectrometer. The profile of the laser focus is imaged by a lens on a CCD camera for monitoring and course preadjustment of the spatial overlap between the beams reflected by the two components of the Mo/Si mirror.

ATR DISPLAYS SINGLE ATTOSECOND X-RAY BURST

Figure 6 summarizes representative results of a series of measurements of streaked X-ray photoelectron spectra recorded with the X-ray and laser pulse impinging with a fixed relative timing set in the X-ray generation process. According to an intuitive one-active-electron model by Schafer *et al.* [20, 21], Corkum [22], and Lewenstein *et al.* [23, 24], ionization of atoms by a linearly polarized laser field is accompanied by emission of extreme-ultraviolet radiation. These theories, along with a number of numerical simulations [24–28], predict that the emission of the highest energy (cutoff) photons will occur near the zero transition(s) of the electric field following the most intense half cycle(s) at the pulse peak in a few-cycle driver.

In a cosine waveform ($\varphi = 0$), cutoff emission is expected to be confined to a single burst emitted at the

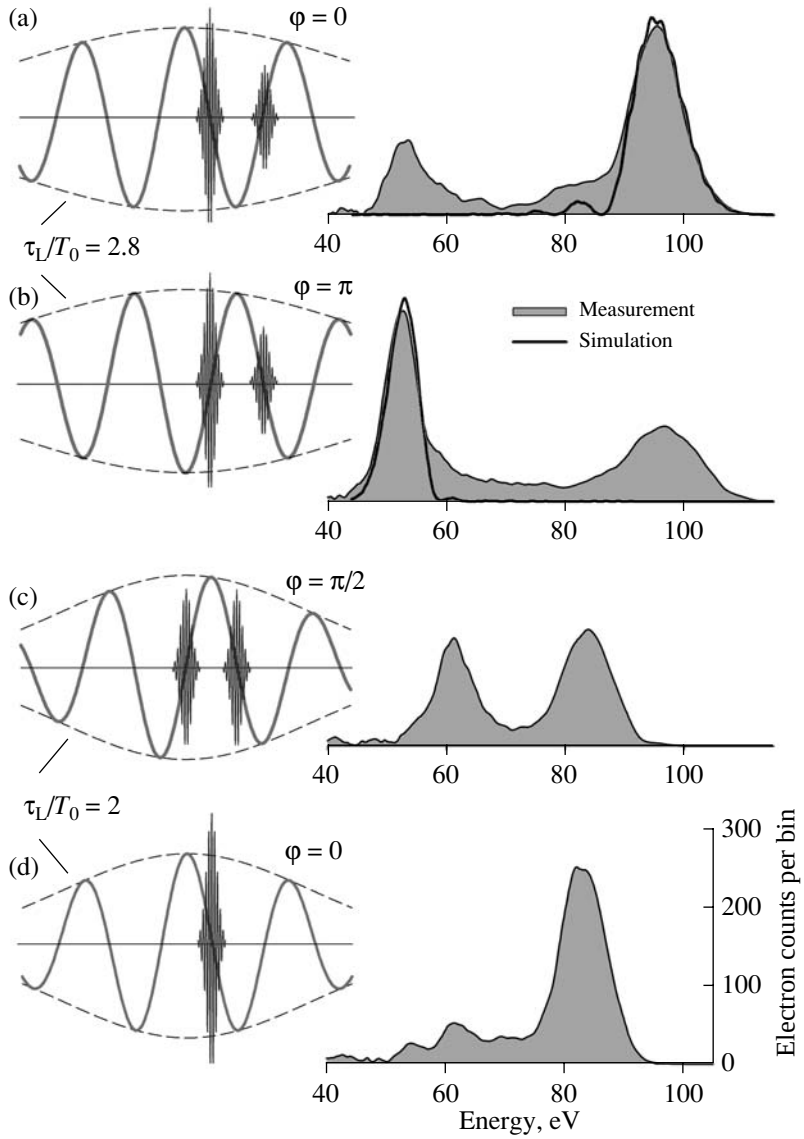

Fig. 6. Streaked photoelectron spectra recorded at the initial delay of the X-ray burst(s) and the (probing) laser light originating from the high-harmonic-generation (HHG) process. The X-ray bursts (blue curves on the left-hand side) originate from the spectrally filtered cutoff energy range of the recombination emission from the HHG neon target pumped by intense few-cycle 750-nm laser pulses (red lines); (a), (b) streaked spectra obtained with laser pulses with a normalized duration of $\tau_L/T_0 = 2.8$ with a cosine and an inverted cosine waveform, respectively. The green curves on the right-hand side depict calculated spectra obtained on the assumption of zero spectral phase (Fourier-limited X-ray burst). The calculations do not model the satellite pulse because the corresponding modulation of the (unperturbed) photoelectron spectrum is insufficiently resolved. (c), (d) Streaked spectra obtained with laser pulses with a normalized duration of $\tau_L/T_0 = 2$ with a sine and a cosine waveform, respectively.

zero transition of $E_L(t)$ following the pulse peak. The photoelectrons ejected in the opposite direction of the peak electric field at this instant undergo a maximum increase of their momentum and, hence, of their energy. The streaked spectrum in Fig. 6d, obtained with 5-fs, 750-nm cosine pulses used for both X-ray generation and subsequent electron streaking, corroborates this prediction. The photoelectron spectrum peaking at $\hbar\omega_{x\text{-}ray} - W_b \approx 72$ eV (where $\hbar\omega_{x\text{-}ray} \approx 93.5$ eV is the center of the X-ray spectrum selected by the Mo/Si mirror, and $W_b = 21.5$ eV is the binding energy of the most weakly bound valence electrons in Ne) in the absence of the laser field is upshifted by about 10 eV with only a few electrons scattered outside the shifted band. The clear upshift is consistent with the X-ray burst coinciding with the zero transition of the laser electric field (see Fig. 6d). Possible satellites would appear at the adjacent zero transitions of $E_L(t)$ and undergo an energy downshift. The absence of a downshifted spectral peak of substantial intensity indicates clean single sub-fs pulse generation.

With the phase adjusted to yield a sine waveform ($\varphi = -\pi/2$), cutoff emission is predicted to come in twin pulses (blue line in Fig. 6c) [2]. The observation of the double-peaked streaked spectrum (Fig. 6c) clearly reflects this time structure.

For the generation of a single sub-fs X-ray burst, the normalized pulse duration τ_L/T_0 plays a crucial role. This is demonstrated by repeating the measurements with slightly longer (7-fs) laser pulses ($\tau_L/T_0 = 2.8$). The corresponding streaked spectrum obtained for $\varphi = 0$ (Fig. 6a) exhibits a sizeable downshifted spectral feature in addition to the upshifted main peak, indicating the appearance of a substantial satellite pulse (≈30% of the principal burst) in the cosine-wave-driven recombination emission. A reduced difference in the intensity of the adjacent half cycles of the few-cycle wave implies that the highest energy spectral components of adjacent bursts reach the energy band selected by our 15%-bandwidth bandpass filter. Shifting φ by π results in the same emission, but the streaking is reversed (Fig. 6b). In these measurements (Figs. 6a and 6b), the strength of the streaking laser field has been increased by a factor of about 2.5.

MEASUREMENT OF THE TIME–MOMENTUM DISTRIBUTION OF THE ELECTRON EMISSION

With isolated sub-fs X-ray pulses at our disposal, atomic transients can now be triggered and their subsequent evolution can be captured by probing the electron emission with a synchronized wave of laser light. For this measurement, the two-component mirror with a delay stage was used to change the timing between the light-field oscillations and the single X-ray burst. Figure 7 shows a series of streaked spectra of photoelectrons emitted from neon as a function of Δt. The excitation pulse at 93 eV was produced by a cosine waveform with $\tau_L/T_0 = 2$.

If the electrons are emitted with an initial kinetic energy much larger than their average quiver energy in the laser field and are temporally confined to a fraction of the half oscillation cycle, theory predicts that their energy shift is linearly proportional to Δp and, hence, to the vector potential at the instant of the release of the wavepacket, as was explained before. As a consequence, $A_L(t)$ and, hence, $E_L(t)$ can be accurately determined from the peak shifts of the spectra—without having to analyze their detailed structure. The result is shown by the black line in Fig. 7, which constitutes the first direct (time-resolved) measurement of a visible light field. With the streaking field $A_L(t)$ known, full temporal (time–momentum) characterization of sub-femtosecond electron emission is now becoming feasible.

First, we are interested in a possible linear frequency sweep carried by the X-ray pulse, because this tends to have a dominant effect on the shape and duration of the excitation. To this end, we analyzed streaked spectra recorded at adjacent zero transitions of $A_L(t)$. These spectra are most sensitive to a linear momentum sweep (caused by a linear frequency sweep of the X-ray pulse), as was explained before. By assuming a possible spectral phase modulation of $\phi_{x\text{-}ray} = \beta_2(\omega - \omega_{x\text{-}ray})^2$ carried by the X-ray pulse and allowing for a timing jitter between the X-ray pulse and the streaking field, we evaluated $\tau_{x\text{-}ray} = 250$ (–5/+30) and $\tau_{jitter} = 260$ (±80). The pulse is found to be essentially Fourier-limited (the near-quadratic frequency sweep results from the asymmetric shape of the pulse spectrum rather than from a spectral phase). The remarkable accuracy of $\tau_{x\text{-}ray}$ relies on using several (in this case, three) projection spectra of the time-momentum distribution of photoelectrons for the X-ray pulse retrieval, which is the essence of the ATR concept. Restricting our analysis to just one of the two streaked spectra would only allow us to set an upper limit of 500 on the X-ray pulse duration. These measurements provide evidence of the emergence of isolated, bandwidth-limited X-ray bursts over a relative spectral band as broad as 15% (15 at 100 eV) from recombination emission driven by a cosine waveform with $\tau_L/T_0 = 2$.

FULL CHARACTERIZATION OF LIGHT WAVES

The ATR's potential for resolving the vector potential $A_L(t)$ of the laser pulse in the time domain made the following measurement an obvious next step. First, some necessary technical improvements had to be made. Mainly, the suppression of vibrations of the vacuum pumps and a new high-quality two-component Mo/Si Mirror with a focal length of 12 cm improved the quality of our measurement. A shift of the photoelectron spectrum by many tens of electronvolts was now readily achievable. The lower inset of Fig. 8 shows a series of spectra obtained by scanning with the X-ray pulse through the laser pulse. From these data, the electric field was retrieved (red curve in Fig. 8), which is also in excellent agreement with a Fourier-limited pulse (gray dashed line) calculated from the laser spectrum. The measurement yielded a pulse duration of 4.3 fs with a maximum field strength of 7×10^7 V/cm [31].

RESOLVING ATOMIC TRANSIENTS WITHIN THE BOHR ORBIT TIME

Quantum-mechanical uncertainty, which dictates that any short-time structure comes with a broad energy spectrum, limits the briefest time interval within which two different atomic events can be recognized as different by the ATR. To be able to resolve the spectral "images" of two events separated by δt in time, they must be shifted with respect to each other in the streak record by at least as much as their own spectral width $\delta W \approx \hbar/\delta t$. From this requirement, we obtain the ATR resolving power:

$$\delta t = \frac{T_0}{2\pi}\sqrt{\frac{\hbar\omega_L}{\Delta W_{max}}}, \qquad (2)$$

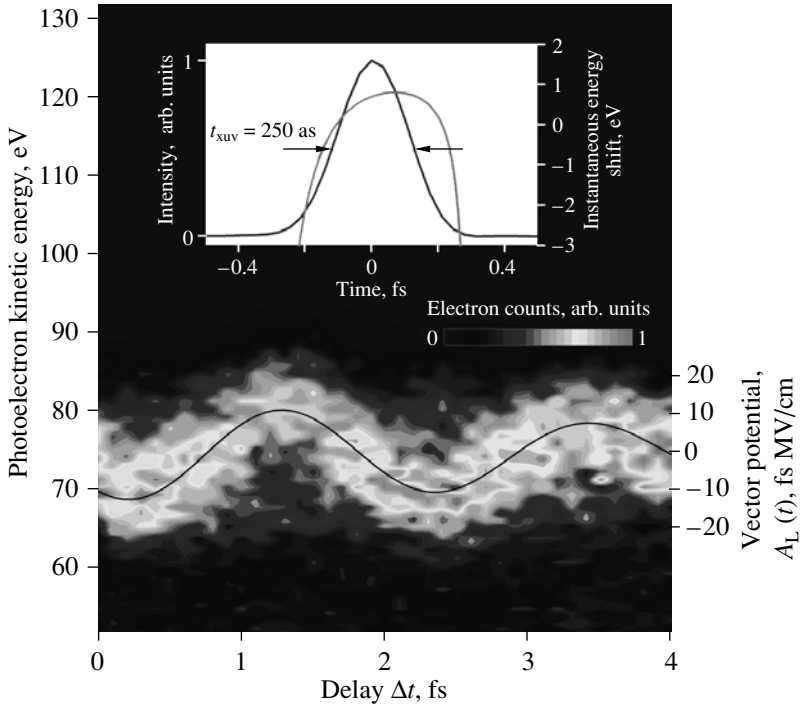

Fig. 7. ATR measurement: a series of projections (streaked kinetic-energy spectra) of the initial time–momentum distribution of photoelectrons ejected by a single sub-fs X-ray pulse. A few-cycle laser pulse with a cosine waveform and a normalized duration of $\tau_L/T_0 = 2$ was used both for generating the single sub-fs excitation pulse and for probing photoelectron emission in the atomic transient recorder. Black line: $A_L(t)$ of the probing field evaluated from the peak shift of the streaked spectra. Inset: Calculated temporal intensity profile and energy sweep of the sub-femtosecond X-ray pulse evaluated from this measurement.

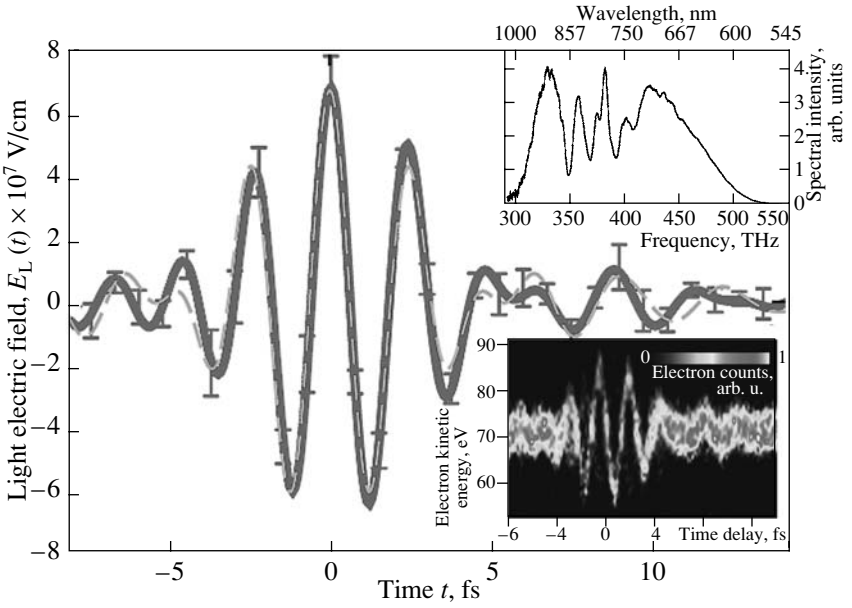

Fig. 8. First complete characterization of the electric field of a light wave in time and space. The electric field was evaluated from recorded electron spectra at different delays between the X-ray and light wave (lower inset) and is in excellent agreement with a Fourier-limited pulse (gray dashed line) retrieved from the spectrum of the laser light wave (upper inset). The measurement yielded a pulse duration of 4.3 fs.

where ΔW_{max} stands for the energy shift suffered by the electron ejected at the peak of $A_L(t)$. Under our current experimental conditions, ΔW_{max} can exceed 20 eV (see Figs. 6a and 6b) before the onset of laser-induced ionization, yielding (for $T_0 = 2$ fs) $\delta t \approx 100$ as. The atomic transient recorder is able to distinguish two ultrafast atomic events following each other within 100 as, which constitutes the shortest interval of time directly measurable to date.

ACKNOWLEDGMENTS

We gratefully acknowledge the invaluable contributions of V. Yakovlev, F. Bammer and A. Scrinzi to the experiments reviewed in this paper.

This work was sponsored by Fonds zur Förderung der wissenschaftlichen Forschung (Austria, grants Z63 and F016), Deutsche Forschungsgemeinschaft (Germany, grants nos. SPP1053, HE1049/9, and KL1077/1) and the European Union's Human Potential Program under contract no. HPRN-2000-00133 (Atto). R. Kienberger is funded by an APART fellowship of the Austrian Academy of Sciences.

REFERENCES

1. A. Zewail, "Femtochemistry: Atomic-Scale Dynamics of the Chemical Bond" (adapted from the Nobel Lecture), J. Phys. Chem. A **104**, 5660–5694 (2000).
2. A. Baltuska *et al.*, "Attosecond Control of Electronic Processes by Intense Light Fields," Nature **421**, 611–615 (2003).
3. T. Brabec and F. Krausz, "Intense Few-Cycle Laser Fields: Frontiers of Nonlinear Optics," Rev. Mod. Phys. **72**, 545–591 (2000).
4. U. Keller, "Recent Developments in Compact Ultrafast Lasers," Nature **424**, 831–838 (2003).
5. M. Drescher *et al.*, "X-ray Pulses Approaching the Attosecond Frontier," Science **291**, 1923–1927 (2001). Published online February 15, 2001; 10.1126/science.1058561.
6. P. M. Paul, E. S. Toma, P. Breger, *et al.*, "Observation of a Train of Attosecond Pulses from High Harmonic Generation," Science **292**, 1689–1692 (2001).
7. Y. Mairesse *et al.*, "Attosecond Synchronisation of High-Harmonic Soft X-Rays," Science **302**, 1540–1543 (2003).
8. P. Tzallas, D. Charalambidis, N. A. Papadogiannis, *et al.*, "Direct Observation of Attosecond Light Bunching," Nature **426**, 267–271 (2003).
9. M. Hentschel *et al.*, "Attosecond Metrology," Nature **414**, 509–513 (2001).
10. C. Wheatstone, Philos. Mag. **6**, 61 (1835).
11. D. J. Bradley, B. Liddy, and W. E. Sleat, Opt. Commun. **2**, 391 (1971).
12. M. Ya. Schelev, M. C. Richardson, and A. J. Alcock, "Image-Converter Streak Camera with Picosecond Resolution," Appl. Phys. Lett. **18**, 354 (1971).
13. J. Itatani, F. Quéré, G. L. Yudin, *et al.*, "Attosecond Streak Camera," Phys. Rev. Lett. **88**, 173903 (2002).
14. M. Kitzler, N. Milosevic, A. Scrinzi, *et al.*, "Quantum Theory of Attosecond XUV Pulse Measurement by Laser-dressed Photoionization," Phys. Rev. Lett. **88**, 173904 (2002).
15. R. Kienberger, E. Goulielmakis, M. Uiberacker, *et al.*, "Atomic Transient Recorder," Nature **427**, 817–821 (2004).
16. D. J. Kane and R. Trebino, "Characterization of Arbitrary Femtosecond Pulses Using Frequency-resolved Optical Gating," IEEE J. Quantum Electron. **29**, 571–579 (1993).
17. T. Sekikawa, T. Katsura, S. Miura, and S. Watanabe, "Measurement of the Intensity-dependent Atomic Dipole Phase of a High Harmonic by Frequency-resolved Optical Gating," Phys. Rev. Lett. **88**, 193902 (2002).
18. M. Drescher *et al.*, "Time-resolved Atomic Inner-Shell Spectroscopy," Nature **419**, 803–807 (2002).
19. A. L'Huillier and P. Balcou, "High-order Harmonic Generation in Rare Gases with a 1-ps 1053-nm Laser," Phys. Rev. Lett. **70**, 774–777 (1993).
20. J. J. Macklin, J. D. Kmetec, and C. L. Gordon III, "High-order Harmonic Generation Using Intense Femtosecond Pulses," Phys. Rev. Lett. **70**, 766–769 (1993).
21. K. J. Schafer, J. L. Krause, and K. C. Kulander, Int. J. Nonlinear Opt. Phys. **1**, 245 (1992).
22. K. J. Schafer, B. Yang, L. F. DiMauro, and K. C. Kulander, "Above Threshold Ionization Beyond the High Harmonic Cutoff," Phys. Rev. Lett. **70**, 1599–1602 (1993).
23. P. B. Corkum, "Plasma Perspective on Strong-Field Multiphoton Ionization," Phys. Rev. Lett. **71**, 1994–1997 (1993).
24. M. Lewenstein, Ph. Balcou, M. Yu. Ivanov, *et al.*, "Theory of High-Harmonic Generation by Low-Frequency Laser Fields," Phys. Rev. A **49**, 2117–2132 (1994).
25. P. Saliéres *et al.*, "Feynman's Path Integral in the Light of Intense-Laser-Atom Experiments," Science **292**, 902–904 (2001).
26. I. P. Christov, M. M. Murnane, and H. C. Kapteyn, "High-Harmonic Generation of Attosecond Pulses in the 'Single-Cycle' Regime," Phys. Rev. Lett. **78**, 1251–1254 (1997).
27. C. Kan, N. H. Burnett, C. E. Capjack, and R. Rankin, "Coherent XUV Generation from Gases Ionized by Several Cycle Optical Pulses," Phys. Rev. Lett. **79**, 2971–2974 (1997).
28. A. de Bohan, P. Antoine, D. B. Milosevic, and B. Piraux, "Phase-dependent Harmonic Emission with Ultrashort Laser Pulses," Phys. Rev. Lett. **81**, 1837–1840 (1998).
29. G. Tempea, M. Geissler, and T. Brabec, "Phase Sensitivity of High-order Harmonic Generation with Few-Cycle Laser Pulses," J. Opt. Soc. Am. B **16**, 669–674 (1999).
30. Terawatt-scale few-cycle pulses recently produced intense recombination emission at 500 eV in the authors' laboratory.
31. E. Goulielmakis, M. Uiberacker, R. Kienberger, *et al.*, "Direct Measurement of Light Waves," Science **305**, 1267–1269 (2004).